Article

The Pierre Auger Observatory: review of latest results and perspectives

Dariusz Gora [1]*[iD] **for the Pierre Auger Collaboration** [2,†,‡]

1   Institute of Nuclear Physics Polish Academy of Sciences, Radzikowskiego 152, Cracow, Poland; Dariusz.Gora@ifj.edu.pl
2   Observatorio Pierre Auger, Av. San Martín Norte 304, 5613 Malargue
*   Correspondence: Dariusz.Gora@ifj.edu.pl
†   auger_spokespersons@fnal.gov
‡   Full author list: http://www.auger.org/archive/authors_2018_07.html

Version October 29, 2018 submitted to Preprints

Abstract: The Pierre Auger Observatory is the world's largest operating detection system for the observation of ultra high energy cosmic rays (UHECRs). The detector allows detailed measurements of their energy spectrum, mass composition and arrival directions of primary cosmic rays in the energy range above 10^{17} eV. The data collected at the Observatory over the last decade show the suppression of the cosmic ray flux at energies above 4×10^{19} eV. However, it is still unclear if this suppression is caused by the propagation of cosmic rays or rather by energy limitation of their sources. The other puzzle is the origin of UHECRs. Some clues can be drawn from studying the distribution of their arrival directions. The recently observed dipole anisotropy has an orientation which indicates an extragalactic origin of UHECRs. The Auger surface detector array is also sensitive to showers due to ultra high energy neutrinos of all flavours and photons, and recent neutrino and photon limits provided by the Observatory can constrain models of the cosmogenic neutrino production and exotic scenarios of the UHECRs origin, such as the decays of super heavy particles. In this paper the recent results on measurements of the energy spectrum, mass composition and arrival directions of cosmic rays, and future prospects are presented.

Keywords: Pierre Auger Observatory; Ultra High Energy Cosmic Rays; Extensive air showers

1. Introduction

The detection of ultra high energy cosmic rays (UHECRs), above 10^{17} eV, is important as it may allow us to answer some of the most important questions in astrophysics: what are the sources of high energy cosmic rays (CRs), where are they produced, what are the corresponding acceleration mechanisms, and what is their elemental composition. In fact, although the existence of UHECRs has been experimentally proven for at least 50 years, these questions are still open, mainly due to the small flux of UHECRs which is one of the reasons for the slow progress in their understanding. The detection of CRs is also important because UHECRs may allow us to probe particle physics at an energy scale beyond TeV energies. When CRs arrive at Earth, they collide with nuclei in the atmosphere at center-of-mass energies which are orders of magnitude above the ones available in man-made particle accelerators. CRs also propagate through the interstellar and intergalactic media and are thus subject to magnetic fields and to interactions with cosmic matter and radiation, therefore having the possibility to provide indirect indications about phenomena which arise only at large distances and highest energies.

Cosmic rays reaching the Earth's atmosphere interact with nuclei, creating a large number of lower energy particles in a showering process. These interactions produce charged pions which can interact or decay, producing both atmospheric neutrinos and high energy muons. Neutral pions decay into gammas, feeding the so-called electromagnetic component of the shower which carries most of the initial energy. Only at the highest energies can showers induced by CRs reach the ground level and be efficiently sampled by an array of surface detectors. Such showers are commonly called Extensive
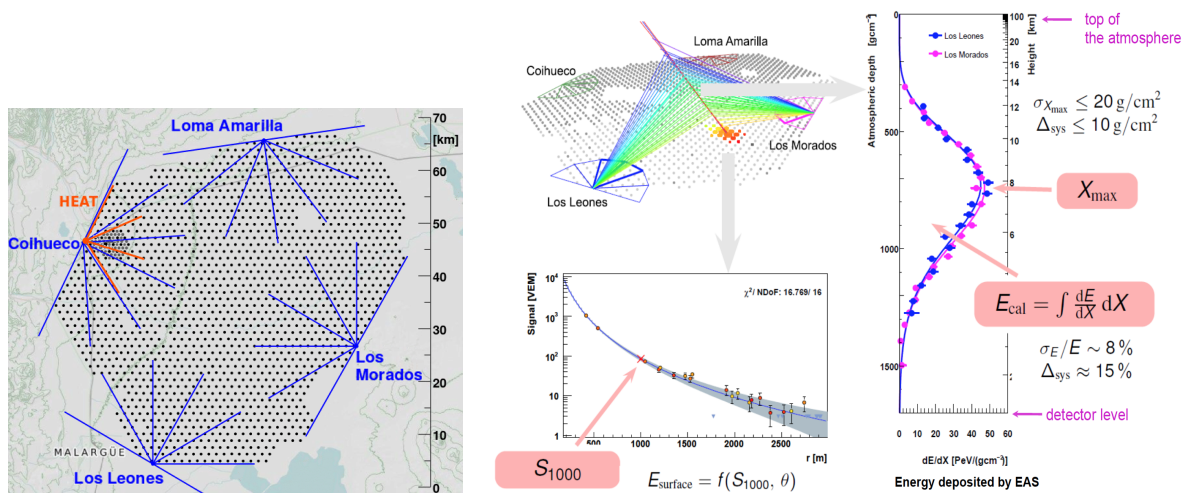
Figure 1. Left: Map of the Pierre Auger Observatory. The four telescope sites are marked in blue with lines indicating the field of view of the telescopes. The surface detector stations are represented by black dots. Right: Example of an event seen simultaneously by the SDs and FDs (hybrid event). The right plot inset shows the measured energy deposit profile of an EAS from the FD, the left plot shows the measured signal from stations of the SD with a fitted lateral distribution function (LDF). The LDF fit allows determining the particle density at a distance 1000 m from the shower axis.

Air Showers (EAS). The electromagnetic component of an EAS produces isotropic fluorescence light by exciting nitrogen molecules in the air. For very high energies of the primary particle, enough fluorescence light is produced by the large number of secondaries in the cascading process so that the shower can be recorded from a distance of many kilometers by an appropriate optical detector system (fluorescence telescopes). As the amount of fluorescence light is correlated with energy dissipated by shower particles, it provides a calorimetric measure of the primary energy.

In this paper after a brief description of the Auger Observatory we report recent results from the Observatory i.e. the measurement of UHECR spectrum, the anisotropy of arrival directions, and on the composition. Finally, also limits on the UHE neutrino flux and limits on the flux of UHE photons are presented.

2. The Pierre Auger Observatory

The Pierre Auger Observatory [1,2] operating since 2004 is the largest project to measure UHECRs. It is located near Malargue in the province of Mendoza, Argentina. It combines a surface array (SD) to measure secondary particles at ground level together with a fluorescence detector (FD) to measure the development of air showers in the atmosphere above the array. Therefore this hybrid detection technique combines the calorimetric measurement of the shower energy through fluorescence light with the high-statistics data of the surface array.

The SD array consists of about 1600 water-Cherenkov detectors arranged in a triangular grid with 1.5 km spacing (SD-1500 array) covering an area of about 3000 km^2. In addition 61 detectors are distributed over 23.5 km^2 on a 750 m grid (SD-750 or 'infill' array), see Figure 1 (left). Each water-Cherenkov detector has three photomultipliers (PMTs) on the top, which sample the shower signal. The signal detected at each station is expressed in a common calibration unit, the so-called vertical equivalent muon or VEM [3]. The SD array is able to collect EAS's at any time with almost 100 % duty cycle.

The fluorescence detector (FD) consists of four telescope buildings (eyes) overlooking the detector array as it is shown in Figure 1 (left). Each building houses 6 telescopes with a $30° × 28.6°$ field of view. The fluorescence light is focused in each telescope onto a camera consisting of 440 PMTs through its Schmidt-optics with a spherical mirror of ~ 13 m^2. The fluorescence detector probes the longitudinal
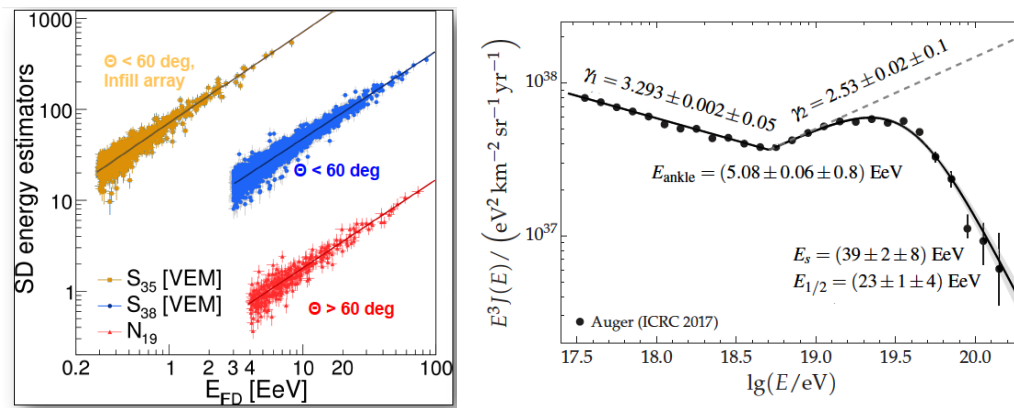
Figure 2. Left: Correlation between the SD energy estimators and the energy measured with the fluorescence telescopes (E_{FD}). The full line is the best fit to data. Right: The Auger energy spectrum with two empirical fit functions (see Ref. [7]). The fitted spectral indices and energies of the break and suppression are superimposed together with their statistical and systematic uncertainties.

development of EAS (Figure 1 (right)) by measuring the photon emission from atmospheric nitrogen, which is excited by shower charged particles. However, it can operate only during clear moonless nights ($\simeq$ 15 % duty cycle). Three additional telescopes pointing at higher elevations (HEAT) are located near one of the FD sites (Coihueco) to detect lower energy showers. An array of radio antennas, the Auger Engineering Radio Array (AERA) [2,4], complements the data with the detection of the shower radiation in the 30-80 MHz region. Details of the design and status of the Observatory can be found in [1,2].

3. Results

3.1. High Energy Cosmic Ray Spectra

The hybrid nature of the Auger Observatory enables us to determine the energy spectrum of primary CRs without strong dependence on our limited knowledge of the mass composition and hadronic interaction models. The Auger approach is to use a selected sample of hybrid events (see Figure 1 (right)) in which the SD energy, E_{SD} can be estimated using the FD. The calibration curves, which are used to find energies of SD events are shown in Figure 2 (left). The parameter chosen to characterize the size of an SD event for the SD-1500 array is the signal at 1000 m from the shower axis, normalized to mean zenith angle of the events of 38° (S_{38}) according to the method described in [5]. For the SD-750 array the mean zenith angle of the events of 35° (S_{35}) is used, while for inclined showers (with the zenith angle larger than 60° seen by SD-1500 array), the (N_{19}) energy estimator is used [6]. Following this method the overall systematic uncertainty of the energy scale remains at 14% [7].

In Figure 2 (right) the Auger combined energy spectrum as presented at ICRC 2017 is shown. The energy spectrum was obtained from the four spectrum components calculated for the hybrid events, events with the SD-1500/SD-750 array and inclined events. The energy spectrum derived from hybrid data is combined with the one obtained from SD data using a maximum likelihood method [8]. From the plot we can see some characteristic features of this combined spectrum: the so-called "ankle" and the flux suppression at highest energies. The position of the ankle at $E_{ankle} = 5.08 \pm 0.06(\text{stat.}) \pm 0.8(\text{syst.})$ EeV has been determined by fitting the flux with a broken power law $E^{-\gamma}$ [7]. An index of $\gamma = 3.293 \pm 0.002(\text{stat.}) \pm 0.05(\text{syst.})$ is found below the ankle. Above the ankle the spectrum follows a power law with index $\gamma = 2.53 \pm 0.02(\text{stat.}) \pm 0.1(\text{syst.})$ with the suppression of the spectrum at $E_s = 39 \pm 2(\text{stat.}) \pm 8(\text{syst.})$ eV. The energy at which the integral flux drops by a factor two below what would be expected without suppression is found to be $E_{1/2} = 23 \pm 1(\text{stat.}) \pm 4(\text{syst.})$
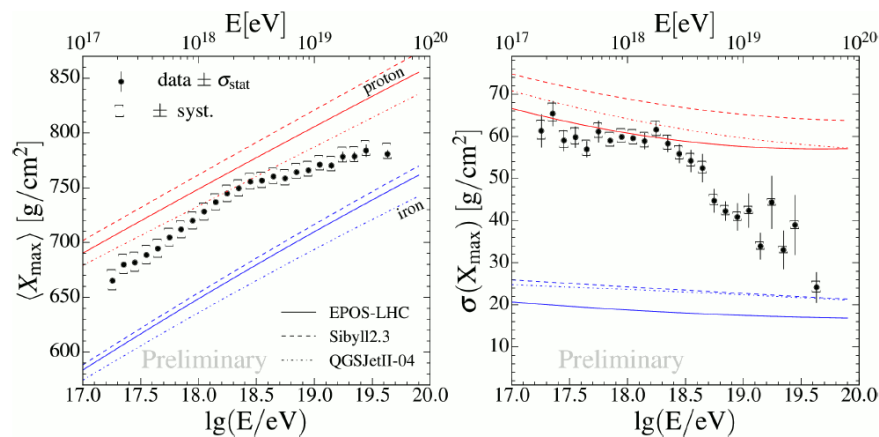
Figure 3. The mean X_{max} (left) and the standard deviation of the X_{max} (right) obtained by the FD as a function of the energy. The predictions of different hadronic interactions models, for pure proton and iron composition, are also shown (see Ref. [12])

EeV. This value is considerably lower than $E_{1/2} = 53$ EeV as predicted for the classical GZK scenario [9] in which the suppression at ultra high energies is caused by depletion of extra-galactic protons during propagation. The suppression of the spectrum can also be described by assuming a mixed composition at the sources or by the limiting acceleration energy at the sources rather than by the GZK-effect [10,11].

3.2. Composition

The atmospheric depth X_{max} where an air shower reaches its maximum size (see as an example Figure 1 (right)) depends on the primary nuclear mass. For a fixed energy, showers initiated by heavy nuclei reach their maximum size on average at smaller X_{max} than those initiated by protons. Shower-to-shower fluctuations in X_{max} are much less for heavy nuclei than for protons. Both of these properties are robust expectations that follow from a heavy nucleus being composed of many nucleons.

In Figure 3 we show the measured $\langle X_{max} \rangle$ and the shower-to-shower fluctuations, $\sigma(X_{max})$ from the Auger Observatory as also presented at ICRC 2017 [12]. The linear fit, $\langle X_{max} \rangle = D_{10} \cdot \lg(E/eV) + c$, yields an elongation rate (variation of $\langle X_{max} \rangle$ per decade of energy) of $D_{10} = 79 \pm 1$ g/cm^2/decade between $10^{17.2}$ and $10^{18.33}$ eV, see Figure 3 (left). This value, being larger than that expected for a constant mass composition (~ 60 g/cm^2/decade), indicates that the mean primary mass becomes lower with increasing energy. At $10^{18.33\pm0.02}$ eV the elongation rate becomes significantly smaller ($D_{10} = 26 \pm 2$ g/cm^2/decade) indicating that the composition becomes heavier with increasing energy. Also the $\sigma(X_{max})$ shows a similar behaviour, see Figure 3 (right). As it can be seen from the plot, the shower-to-shower fluctuations decrease from 60 g/cm^2 to about 30 g/cm^2 as the energy increases. This decreasing fluctuations are an independent signature of increasing average mass of the primary particles.

The Auger X_{max} data (distributions and their moments) enable a step further in the interpretation of mass composition by studying the evolution of the first two moments of $\ln A$ with energy [12,13,15] as well as the evolution of the fractions of four mass groups (H, He, N and Fe) obtained from the fit of the X_{max} distributions [12–15]. The latest results are shown in Figure 4. At the lowest energies, we find hints for a contribution (25-38 % depending on hadronic interaction model used) from iron primaries that disappears rapidly with increasing energy. At higher energies the composition is dominated by different elemental groups, starting from protons below the ankle and going through helium to nitrogen as the energy increases. This evolution occurs with apparently limited mass mixing as a consequence of the small values of the X_{max} dispersion. The interpretation of X_{max} data depends on the hadronic interaction model. In particular QGSJETII-04 appears to be less consistent with data as can be seen in the lower panel of Figure 4, where the p-value of the fit is shown. This is because
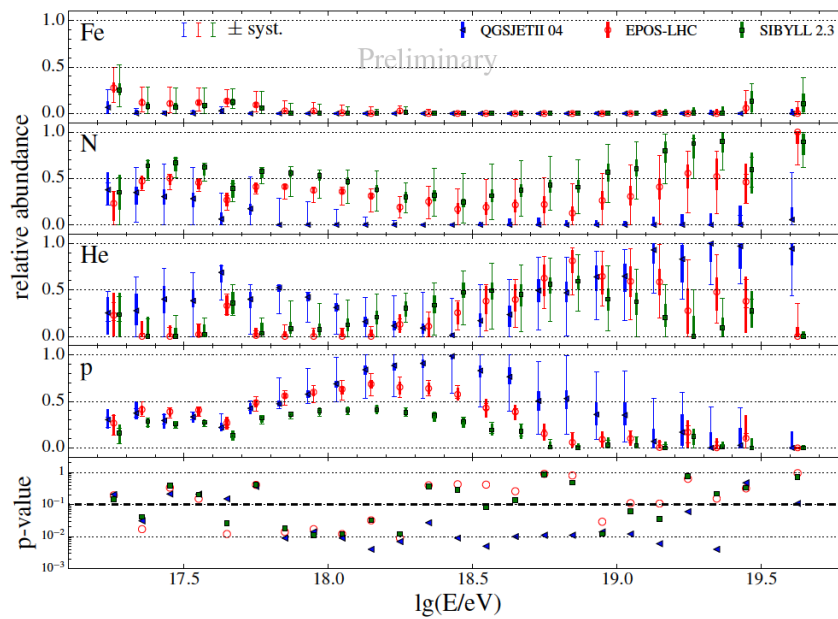
Figure 4. Mass fraction fits obtained using parameterizations of the $X_{\max}$ distributions from the fluorescence $X_{\max}$ data. The error bars indicate the statistics (smaller cap) and the systematic uncertainties (larger cap). The bottom panel indicates the goodness of the fits (p-values), see [12] for more details.

the present interpretation relies on air shower simulations that use hadronic interaction models to extrapolate particle interaction properties over two orders of magnitude in center-of-mass energy beyond the regime where they have been tested experimentally. The possible different interpretation can be that the proton-air interaction cross section or multiplicity, or both, are increased leading to a faster shower development, as would happen in heavy nuclei collisions [12] . In other words, the precise interpretation of the Auger X_{max} and $\sigma(X_{max})$ result is still an open question.

3.3. Anisotropy

An anisotropy in the arrival direction distribution of CRs in the energy range of the GZK suppression is expected because of the highly anisotropic matter distribution on distance scales of 100 Mpc. The extragalactic magnetic fields are not strong enough to deflect significantly high energy cosmic rays during their propagation to the Earth, so the observed source distribution in principle should reflect the matter distribution in the nearby universe. The Auger Collaboration has undertaken several anisotropy searches at different energy ranges and angular scales. These use several tools like harmonic analysis, auto-correlation, correlation with source catalogs, and search for flux excesses in the visible sky and correlations with other experiments.

Among the most recent studies the most exciting result is the observation of a large-scale anisotropy in the arrival directions of CRs above 8×10^{18} eV [16]. Two energy bins, 4 EeV< $E \leq 8$ EeV and $E \geq 8$ EeV, were analyzed in data obtained since the start of data taking with the Observatory (total exposure of 76,800 km^2 sr yr) to determine the amplitude of the first harmonic in right ascension, Figure 5 (left). The right ascension anisotropy found in the two energy bins has amplitudes $0.5^{+0.6}_{-0.2}$ % and $4.7^{+0.8}_{+0.7}$ %, respectively. The events in the lower energy bin follow an arrival direction distribution consistent with isotropy, but in the higher energy bin a significant anisotropy was found, with a p-value of 2.6×10^{-8} under the isotropic null hypothesis. The three-dimensional dipole, obtained by combining the first-harmonic analysis in right ascension with a similar one in the azimuthal angle, has a direction in galactic coordinates (l, b) = ($233°$, $-13°$) which is about $125°$ away from the Galactic Centre. Hence this anisotropy indicates an extragalactic origin for these UHECR particles. The dipole
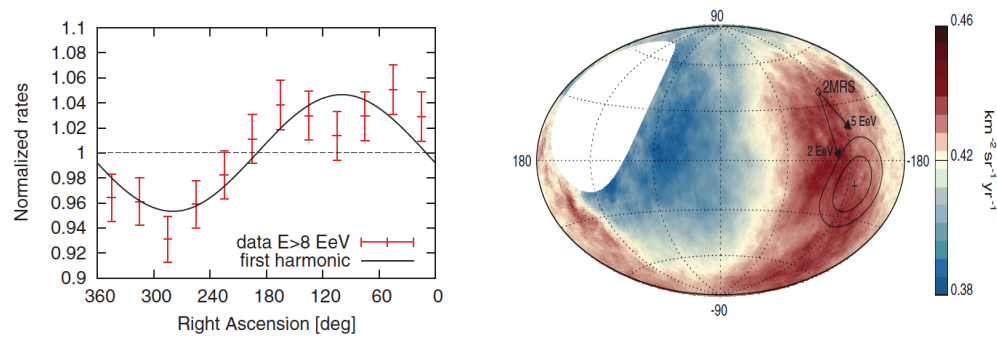
Figure 5. Left: Normalized rate of events as a function of right ascension for $E \geq 8$ EeV. The error bars represent 1σ uncertainties [16]. Right: Sky map in galactic coordinates of the cosmic ray flux for $E \geq 8$ EeV. The cross indicates the dipole direction and the contours mark the 68 % and 95 % confidence level regions [16]. The diamond marks the dipole direction of the 2MRS galaxy distribution [17]. The arrows show the deflections expected from the model described in [18] for particles with $E/Z = 5$ or 2 EeV.

152 anisotropy has an amplitude of $6.5^{+1.3}_{-0.9}\%$ and level of significance of 5.2 σ. A skymap of the intensity of
153 CRs arriving above 8 EeV is shown in Figure 5 (right).

3.4. Photons and neutrinos

155 Another important issue concerning composition studies is the search for photons and neutrinos
156 in primary CRs. Photons and neutrinos may directly trace back the origin of the UHECR. Essentially all
157 models of UHECRs production predict neutrinos/photons as a result of the decay of charged/neutral
158 pions produced in interactions of CRs within the sources themselves or while propagating through
159 background radiation fields. For example, UHECR protons interacting with the cosmic microwave
160 background (CMB) give rise to the so-called "cosmogenic" or GZK neutrinos [19]. The cosmogenic
161 neutrino flux is somewhat uncertain since it depends on the primary UHECR composition and on the
162 nature and cosmological evolution of the sources as well as on their spatial distribution. In general,
163 about 1 % of cosmogenic neutrinos is expected in the ultra high energy cosmic ray flux.
164 Due to their low interaction probability, neutrinos need to interact with a large amount of mat
165 ter in order to be detected. One of the detection techniques is based on the detection of EAS in the
166 atmosphere by looking for very inclined young showers. The neutrino events would have a significant
167 electromagnetic component leading to a broad time structure of the detected signal, in contrast to
168 nuclei-induced showers.
169 When propagating through the Earth, only the so-called Earth skimming (ES) tau neutrinos may
170 initiate detectable air showers above the ground [20,21]. In this case tau neutrinos may interact within
171 the Earth and produce charged tau leptons which in turn decay into neutrinos with lower energies.
172 Since the interaction length for the produced tau lepton is a few tens kilometers at the energy of about
173 1 EeV, the leptons produced close to the Earth's surface may emerge from the ground, decay in air and
174 produce EAS potentially detectable by the surface detector of the Auger Observatory [22]. The SD
175 is also sensitive to down-going neutrinos (DG) in the EeV energy range. Down-going neutrinos of
176 any flavour may interact through both charged (CC) and neutral current (NC) interactions, producing
177 hadronic and/or electromagnetic showers, see [22] for details about the search technique. Up to now,
178 no candidate events have been found by the Auger Observatory to fulfill the selection criteria. The
179 absence of neutrino candidate events yields an upper limit on the diffuse flux of neutrinos in the EeV
180 energy range [22], see Figure 6 (left).
181 The Auger Observatory has also set new photon limits with both the hybrid and SD detection
182 methods [23,24]. The new limits are compared to previous results and to theoretical predictions in
183 Figure 6 (right). In terms of the photon fraction, the current bound at 10 EeV approaches the percent
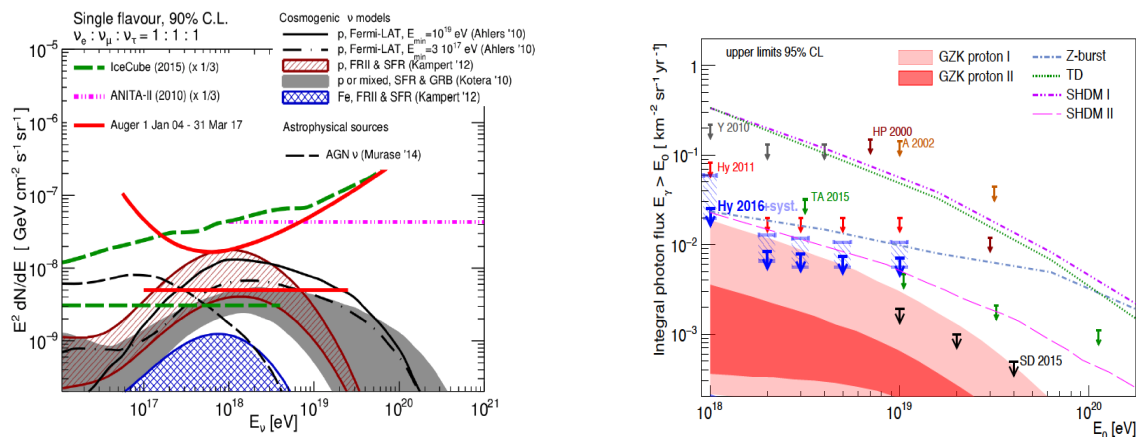
Figure 6. Left: Differential (curved red line) and integrated (straight red line) upper limits (90 % C.L.) from the Pierre Auger Observatory for a diffuse flux of neutrinos in the period 1 Jan 2004 - 31 March 2017. The limits are drawn for a single flavor, assuming equal flavor ratios. Limits from ANITA (magenta dotted dashed line), and IceCube (green dashed line), along with several model predictions are also shown, see [22] for the complete set of references. Right: Upper limits on the integrated photon flux, along with several model predictions. The bold arrows (Hy 2016) correspond to the most recent data analysis in Auger using hybrid events, the blue dashed boxes mark the systematic uncertainties of this study. The limits of previous studies done by Auger, Hy2011 (red arrows), and SD 2015 (black arrows), the latter one using only SD data, are also shown. The results from other experiments are also presented. See [23,24] for the complete set of references.

184 level while previous bounds were at the 10 percent level. A discovery of a substantial photon flux
185 could have been interpreted as a signature of top-down (TD) models. In turn, the experimental limits
186 now put strong constraints on these models.

187 *3.5. Multi-messenger astronomy*

188   The Pierre Auger Observatory actively participates in multi-messenger searches in collaboration
189 with other observatories. So far, searches for correlation of arrival directions of CRs detected by the
190 Telescope Array and Auger collaborations, with arrival directions of neutrino events detected by
191 IceCube have been performed [25]. No indications of correlations at discovery level were found.
192 The detection of the first Gravitational Wave (GW) transient GW150914 on September 14, 2015, by
193 the Advanced LIGO detectors opened a new era in multi-messenger astronomy [26], enhancing the
194 participation of many other experiments, of which the Pierre Auger Observatory is also a part. Auger
195 performed neutrino searches in coincidence with the gravitational wave events GW150914, GW151226,
196 LVT15012 [27], and GW170817/GRB 170817A [28]. The GW170817/GRB 170817A [29], a gravitational
197 wave event detected on August 17, 2017, was later observed as a short gamma-ray burst by the
198 Fermi-GBM and INTEGRAL. This event was caused by the merging of a binary of neutron stars in the
199 host galaxy NGC4993 at a distance of 40 Mpc, the closest gravitational event detected so far. Neutrino
200 searches related to this event were carried out by the three most sensitive neutrino observatories
201 IceCube, Antares and Auger. The sky map of these neutrino searches is shown in Figure 7. In Auger,
202 the whole ± 500 s time window was observed in the ES channel field of view. No inclined showers
203 passing the ES channel selection were detected during this period. Assuming neutrinos are emitted
204 steadily during this period, with an energy spectrum of E^{-2} [27], the non-detection of candidates
205 allows us to put limits to neutrino fluence, see Figure 7 (right). In the following 14 days, searches were
206 done both in the ES and DG channels. No neutrino candidates were found in this time window either.
207 No significant counterpart was found in any of the searches with any of the observatories, a result
208 which is compatible with the expectations of a GRB observed off-axis, Figure 7 (right).
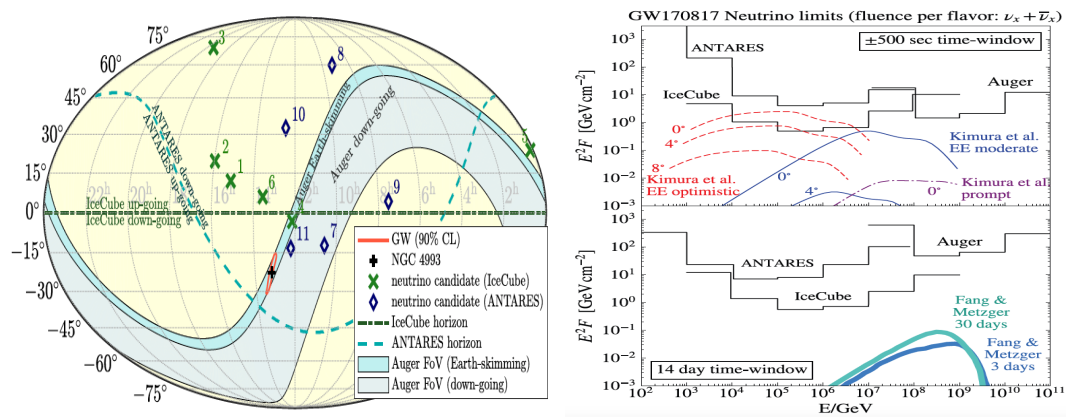
Figure 7. (Left) Sensitive sky areas of ANTARES, IceCube and Auger at the time of the GW170817 event in Equatorial Coordinates [27]. (Right): Upper limits at 90% C.L. of the neutrino spectral fluence from GW1700817 event for a 500s time window (top panel) and in the following 14 days after the trigger (bottom panel) [27].

3.6. Auger Prime

Taking stable data since 2004, the Pierre Auger Collaboration has published many results about properties of UHECRs. Among the latest results at the highest energies using SD data, the extragalactic origin of cosmic rays with E > 8 EeV [16] was established. However, to identify the UHECR sources, it is crucial to determine the nuclear mass composition in the flux suppression energy region. Unfortunately, the low duty cycle of the FD does not allow collecting a significant data sample for energies above $10^{19.6}$ eV [12]. Several other mass composition analyses using the SD were performed by the Pierre Auger Collaboration, but these suffer from larger systematic uncertainties due to the uncertainties in the assessment of the muon content of the shower using the water-Cherenkov detectors. Thus it is also difficult to build a consistent picture of the origin of UHECRs.

To address such challenges, the Pierre Auger Observatory is currently undergoing a major upgrade phase, called AugerPrime [30]. The key upgrade element is the installation of a 4 m^2 plastic scintillator detector on top of each of the 1660 water-Cherenkov stations (Figure 8), enabling a better discrimination between the electromagnetic and muonic components of the shower. Additionally, the duty cycle of the fluorescence telescopes will be extended, allowing a direct determination of the depth of shower maximum with increased statistics at the highest energies. The electronics of the SD stations is being upgraded to obtain an increased sampling rate and a better timing accuracy, as well as a higher dynamic range, allowing a better reconstruction of the geometry of the showers.

The first step for ongoing upgrade is the AugerPrime Engineering Array (EA) [31], which consists of 12 upgraded detector stations already operational since 2016. With this setup we have verified the basic functionality of the detector design, the linearity of the scintillator signal, the calibration procedures and operational stability. The construction of AugerPrime is expected to be finished in 2019 and it will be followed by data-taking until 2025.

4. Conclusions

The measurements performed at the Pierre Auger Observatory indicate a change in the nature of cosmic rays at around 3 EeV and show a change in the shape of the energy spectrum and of the elongation rate. These measurements add support to the hypothesis that an extragalactic component of mixed composition starts to dominate in this energy range. The recently observed dipole anisotropy has an orientation which indicates an extragalactic origin of UHECRs. The near future particle accelerator results and AugerPrime will constrain the hadronic interaction models so that the interpretation of the evolution of the shower maximum with energy will be more conclusive. The photon limits exclude most of the top-down scenarios above 2 EeV, and the neutrino limits, if no neutrino is observed,

will improve by more than an order of magnitude. These determinations, together with the arrival directions and mass composition analysis will help in solving the puzzle of the origin of the highest energy cosmic rays.
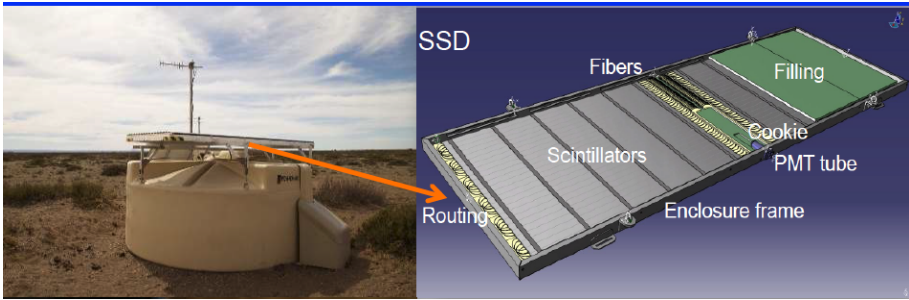

Figure 8. The picture of one upgraded station (left) and the layout of the Surface Scintillator Detector (right).

Abbreviations

The following abbreviations are used in this manuscript:

UHECRs	ultra high energy cosmic rays
CRs	cosmic rays
SD	surface detector
FD	fluorescence detector
ES	earth skimming
DG	down-going
EAS	extensive air shower

References

1. Abraham, J., et al. Properties and performance of the prototype instrument for the Pierre Auger Observatory. *Nucl. Instrum. Meth.* **2004**, *A523*, 50, doi:10.1016/j.nima.2003.12.012

2. Aab, A., et al. The Pierre Auger Cosmic Ray Observatory. *Nuclear Instruments and Methods in Physics Research A* **2015**, *798*, 172, doi:10.1016/j.nima.2015.06.058

3. Abraham, J., et al. Trigger and Aperture of the Surface Detector Array of the Pierre Auger Observatory. *Nucl. Instrum. Methods A* **2010**, *613*, 29, doi:10.1016/j.nima.2009.11.018

4. Abreu, P., et al. Antennas for the Detection of Radio Emission Pulses from Cosmic-Ray induced Air Showers at the Pierre Auger Observatory. *JINST* **2012**, *437 (7)*, P10011, doi:10.1088/1748-0221/7/10/P10011

5. Abraham, J., et al. Observation of the suppression of the flux of cosmic rays above 4×10^{19} eV. *Phys. Rev. Lett.* **2008**, *101*, 061101

6. Aab, A., et al. Reconstruction of inclined air showers detected with the Pierre Auger Observator. *JCAP* **2014**, *08*, 16, doi:10.1088/1475-7516/2014/08/019

7. Fenu, F., et al. The cosmic ray energy spectrum measured using the Pierre Auger Observatory. *PoS(ICRC2017)* **2017** *486*

8. Aab, A., et al. Measurement of the energy spectrum of cosmic rays above 10^{18} eV using the Pierre Auger Observatory. *Phys. Lett. B* **2010**, *685*, 239, doi:10.1016/j.physletb.2010.02.013

9. Berezinsky, V. S., Gazizov, A. Z., Grigorieva, S. I. On astrophysical solution to ultra high energy cosmic rays. *Phys. Rev. D* **2006**, *74*, 043005

10. Greisen, K. End to the Cosmic-Ray Spectrum? *Phys. Rev. Lett.* **1966**, *16* , 748, doi:10.1103/PhysRevLett.16.748

11. Zatsepin, G.T., Kuz'min, V.A. Upper limit of the spectrum of cosmic rays. *J. Exp. Theor. Phys. Lett.* **1966** *4* 78

12. Bellido, J., et al. Depth of maximum of air-shower profiles at the Pierre Auger Observatory: Measurements above $10^{17.2}$ eV and Composition Implications. *PoS(ICRC2017)* **2017**, *506*, doi:10.22323/1.301.0506

13. Aab, A., et al. Depth of maximum of air-shower profiles at the Pierre Auger Observatory. I. Measurements at energies above 10e17 eV. *Phys. Rev. D* **2014**, *90*, 122005, doi:10.1103/PhysRevD.90.122005

14. Aab, A., et al. Depth of maximum of air-shower profiles at the Pierre Auger Observatory. II. Composition implications. *Phys. Rev. D* **2014**, *90*, 122006, doi: 10.1103/PhysRevD.90.122006

15. Aab, A. et al. The Pierre Auger Observatory: Contributions to the 35th International Cosmic Ray Conference (ICRC 2017). **2017** arXiv:1708.06592

16. Aab, A., et al. Observation of a Large-scale Anisotropy in the Arrival Directions of Cosmic Rays above $8 \cdot 10^{18}$ eV *Science* **2017**, *357*,1266,doi:10.1126/science.aan4338

17. Erdoğdu, P. The dipole anisotropy of the 2 Micron All-Sky Redshift Survey. *Mon. Not. R. Astron. Soc.* **2006**, *368*, 1515, doi: 10.1111/j.1365-2966.2006.10243.x

18. Jansson, R., Farrar, G.R. A New Model of the Galactic Magnetic Field. *Astrophys. J.* **2012**, *757*, 14, doi:10.1088/0004-637X/757/1/14

19. Beresinsky, V.S., Zatsepin G.T. Cosmic rays at ultra high energies (neutrino?). *Physics Letters B* **1969**, *28*, 423, doi:10.1016/0370-2693(69)90341-4

20. Fargion, D. Discovering Ultra High Energy Neutrinos by Horizontal and Upward tau Air-Showers: Evidences in Terrestrial Gamma Flashes? *Astrophys.J.* **2002**, *570*, 909, doi:10.1086/339772

21. Bertou, X., et al. Tau Neutrinos in the Auger Observatory: A New Window to UHECR Sources. *Astropart. Phys.* **2002**, *17*, 183, doi:10.1016/S0927-6505(01)00147-5

22. Zas, E., et al. Searches for neutrino fluxes in the EeV regime with the Pierre Auger Observatory. *PoS(ICRC2017)* **2018**, *972*, doi:10.22323/1.301.0972

23. Niechciol, M., et al. Diffuse and targeted searches for ultra high-energy photons using the hybrid detector of the Pierre Auger Observatory. *PoS(ICRC2017)* **2018**, *517*

24. Aab., A., et al. Search for photons with energies above 10^{18} eV using the hybrid detector of the Pierre Auger Observatory. *JCAP* **2017**, *04* , 9, doi:0.1088/1475-7516/2017/04/009

25. Aartsen, A., et al. Search for correlations between the arrival directions of IceCube neutrino events and ultra high-energy cosmic rays detected by the Pierre Auger Observatory and the Telescope Array. *JCAP* **2016**, *01* , 037, doi:10.1088/1475-7516/2016/01/037

26. Abbott, B.P. et al. Observation of Gravitational Waves from a Binary Black Hole Merger. *Phys. Rev. Lett.* **2016**, *116*, 061102, doi:10.1103/PhysRevLett.116.061102

27. Aab, A., et al. Ultra high-energy neutrino follow-up of gravitational wave events GW150914 and GW151226 with the Pierre Auger Observatory. *Phys. Rev. D* **2016**, *94* 122007, doi: 10.1103/PhysRevD.94.122007

28. Albert, A. et al. Search for High-energy Neutrinos from Binary Neutron Star Merger GW170817 with ANTARES, IceCube, and the Pierre Auger Observatory. *Astrophys. J.* **2017**, *850*, L35, doi:10.3847/2041-8213/aa9aed

29. Abbott, B. P. et al. Multi-messenger Observations of a Binary Neutron Star Merger. *ApJL* **2017**, *848*, L12, doi:10.3847/2041-8213/aa91c9

30. Aab, A., et al. The Pierre Auger Observatory Upgrade - Preliminary Design Report, arXiv:1604.03637 **2016**

31. Martello, D. et al. The Pierre Auger Observatory Upgrade. *PoS(ICRC2017)* **2017**, *383*